Semiclassical theory of quantum stochastic resistors

Tony Jin,[1] João Ferreira,[1] Michel Bauer,[2,3] Michele Filippone,[4] and Thierry Giamarchi[1]

[1]*Department of Quantum Matter Physics, École de Physique University of Geneva, Quai Ernest-Ansermet 24, CH-1211 Geneva 4, Switzerland*

[2]*Université Paris-Saclay, CNRS, CEA, Institut de Physique Théorique, 91191 Gif-sur-Yvette, France*

[3]*PSL Research University, CNRS, École normale supérieure, Département de mathématiques et applications, 75005 Paris, France*

[4]*Univ. Grenoble Alpes, CEA, Grenoble INP, IRIG-MEM-L_Sim, Grenoble, France*

(Received 30 June 2022; revised 14 November 2022; accepted 13 December 2022; published 23 January 2023)

We devise a semiclassical model to describe the transport properties of low-dimensional fermionic lattices under the influence of external quantum stochastic noise. These systems behave as *quantum stochastic resistors*, where the bulk particle transport is diffusive and obeys the Ohm/Fick's law. Here, we extend previous exact studies beyond the one-dimensional limit to ladder geometries and explore different dephasing mechanisms that are relevant to different physical systems, from solid-state to cold atoms. We show how the semiclassical description is useful to explain the nontrivial dependence of the conductance of these systems on the chemical potential of the reservoirs. This description provides an intuitive and simpler interpretation of transport in quantum stochastic resistors in good quantitative agreement with the exact numerical solution. Moreover, we find that the conductance of quantum ladders is insensitive to the coherence of the dephasing process along the direction transverse to transport, despite the fact that the system reaches different stationary states.

DOI: 10.1103/PhysRevResearch.5.013033

I. INTRODUCTION

Diffusion is the most common type of transport encountered in many-body systems, both in the classical and in the quantum world. In condensed matter setups, it is observed whenever the resistance of a metallic conductor is measured. The emergence of resistive behavior is commonly attributed to the diffusive propagation of charge carriers caused by scattering with disorder, impurities or particles of the same or different nature (electrons, holes, phonons, magnons, etc.) [1]. Despite the clarity of these physical mechanisms, describing the emergence of diffusive transport from a full quantum perspective remains an open issue in theoretical physics [2–8].

In recent years, the study of open quantum systems has opened new exciting venues to understand the emergence of diffusion. The Markovian description of leads [9–16], losses [17–20] or external time-dependent noises [15,21–31] has provided valuable numerical and analytic insight into the problem. In this context, dephasing has been in the spotlight for being an analytically tractable process of physical importance. It is capable of describing the emergence of diffusion in quantum coherent systems [15,32–34], which behave as *quantum stochastic resistors* [35].

Despite these exact derivations of classical diffusive transport in the quantum realm, it remains an open question to which extent a classical description can account for the coherent transport properties and with which accuracy [36–38]. If successful, a classical description could provide additional insight on transport phenomena outside the framework of open quantum systems.

Moreover, most of the studies mentioned above are restricted to one dimension, often exploiting integrable structures in some fine tuned cases [8,22,32,39]. It is thus important to investigate the extension of exact solutions to higher dimensions and their richer behavior [40]. This understanding is also relevant to open new perspectives in the context of quantum matter simulators, where controlled dissipative dynamics is under study in both bosonic [41–43] and fermionic systems [44,45].

In this paper, we devise a semiclassical model, which accurately describes the transport properties of one-dimensional quantum stochastic resistors. We then derive a set of conditions under which the result for the 1D conductance can be extended to 2D systems. We focus on the quantum ladders geometries sketched in Fig. 1 (top), where a current is driven by a difference of chemical potential $\delta\mu$ between thermal leads. The lattice is under the influence of dephasing processes and the working principle of the semiclassical model is illustrated in Fig. 1 (bottom), in the one-dimensional limit. Semiclassically, dephasing is conceived as a stochastic reset of single particle velocities, which mimics a series of random quantum measurements of the particle position.

To characterize the transport properties of a dephased chain, we consider their conductance at a weak bias $\delta\mu$. We show that, in the presence of dephasing, the conductance is suppressed with the longitudinal extent of the system—the number of sites N in Fig. 1 (top)—revealing the emergence of bulk resistivity. We also observe that dephasing triggers a nontrivial dependence of the conductance on the chemical

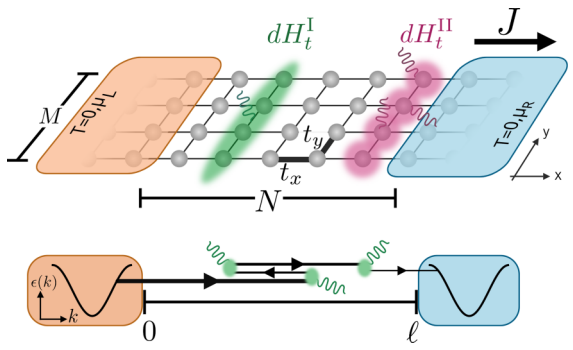

FIG. 1. (Top) Schematic representation of the system under study. An M-leg square ladder is attached at the edges to two leads prepared at the same temperature with distinct chemical potentials $\mu_{\mathrm{L,R}}$. The bias $\delta\mu$ in the chemical potential drives a particle current J that can depend on the noise. Noises differ on the spatial correlation along the y direction ranging from uniformly correlated dH_t^{I} to uncorrelated dH_t^{II}. (Bottom) Semiclassical interpretation of a 1D diffusive channel. A particle leaves a lead with a velocity determined by the band dispersion. A reset of a particle's velocity occurs at random times until it escapes to one of the leads. The distance between leads is $\ell = Na$ with a the lattice spacing.

potential μ of the reservoirs. In particular, the conductance vanishes when the chemical potential approaches the band edges, reflecting a suppression with the velocity of particles injected by the reservoirs. This dependence is absent in the ballistic case and is particularly intriguing as it is also absent in the bulk diffusion constant of the system. We show then how the semiclassical model is able to accurately reproduce the emergent μ dependence of the conductance, providing at the same time a simple physical picture connecting boundary and bulk diffusive effects.

We then extend these considerations to ladder systems. The presence of an additional degree of freedom along the y direction, transverse to the current flow along x, allows different dephasing processes. These processes can be either coherent or incoherent along the y direction, see Fig. 1 (top). The coherent case is for instance relevant to cold atom systems with a synthetic y dimension [46–49]. Even though these different noises drive the system towards totally different stationary states, we find that they carry exactly the same current. We explain this remarkable coincidence as a manifestation of the fact that the correlations of these different noises obey identical isotropy conditions, that we derive and discuss in detail.

This paper is structured as follows. In Sec. II, we discuss the Keldysh approach for the exact self-consistent derivation of currents in quantum stochastic ladder resistors. Section III introduces the semiclassical approach and illustrates its ability to reproduce exact results. Section IV discusses the extension to ladders and Sec. V discusses results and conclusions.

II. MODEL AND METHODS

We study the transport properties of spinless fermions on the discrete square lattice geometry sketched in Fig. 1 (top). We consider an infinite lattice along the longitudinal direction (x axis), with M sites in the transverse direction (y axis). The corresponding Hamiltonian reads

$$H = -\sum_{j,m}[t_x c^\dagger_{j+1,m} c_{j,m} + t_y c^\dagger_{j,m+1} c_{j,m} + \mathrm{H.c}]\,, \qquad (1)$$

where the sum over j runs between $\pm\infty$ and the second index between 1 and M. The operators $c_{j,m}$ annihilate fermions on site (j,m) and $t_{x/y}$ control the hopping amplitude along the x/y directions. We further divide the sum over the longitudinal direction into three regions: the system (S) for $j \in [1,N]$, the left (L) lead for $j<1$ and the right (R) lead for $j>N$, see Fig. 1 (top). It is useful to introduce the basis diagonalizing the transverse hopping term in Eq. (1), given by the unitary transformation $a_{j,p} = \sum_{m=1}^{M}\sqrt{\frac{2}{M+1}}\sin(\frac{\pi mp}{M+1})c_{j,m}$. This transformation uncouples the M transverse modes and the corresponding Hamiltonian reads

$$H = \sum_{j,p}[-t_x(a^\dagger_{j+1,p}a_{j,p} + \mathrm{H.c}) + \epsilon_p a^\dagger_{j,p}a_{j,p}]\,, \qquad (2)$$

with $\epsilon_p = -2t_y\cos(p\pi/(M+1))$ and $p\in[1,M]$. If the system is translational invariant along the x direction, the transverse modes have nondegenerate dispersion relations $\epsilon_{p,k} = -2t_x\cos(k)+\epsilon_p$, with $k\in[-\pi,\pi]$ the quasimomentum in the first Brillouin zone, see sketches in Fig. 3 for an illustration in the $M=2$ case. We reserve the indexes j,m for the physical sites in the x and y direction, and the indexes k,p label respectively longitudinal quasi-momenta and transverse modes.

In addition to the coherent Hamiltonian dynamics, we introduce a noise term modelled by a quantum stochastic Hamiltonian (QSH) that leads to various dephasing mechanisms that we are going to detail. The QSH is defined by the infinitesimal generator dH_t such that the total unitary operator $U(t)$ is evolved as

$$U(t+dt) = e^{-i(Hdt+dH_t)}U(t)\,. \qquad (3)$$

In this paper, we are interested in QSHs, which conserve the total particle number and lead to dephasing. They are described by

$$dH_t = \sqrt{2\gamma}\sum_{j,p,p'} a^\dagger_{j,p}a_{j,p'}dW_t^{j,p,p'}\,, \qquad (4)$$

where γ controls the overall dephasing rate and the dW_t are increments of stochastic processes defined within the Itō prescription [50]. The noise have a 0 mean, $\mathbb{E}[dW_t = 0]$ and their Itō rules are defined to be

$$dW_t^{j_1,p_1,p_1'}dW_{t'}^{j_2,p_2,p_2'} = \delta_{j_1,j_2}C_{p_1,p_1',p_2,p_2'}dt \quad \text{for } t=t',$$
$$dW_t^{j_1,p_1,p_1'}dW_{t'}^{j_2,p_2,p_2'} = 0 \quad \text{for } t\neq t'. \qquad (5)$$

By construction, the noise is thus uncorrelated in time and in the longitudinal x direction, j index, but not necessarily on the transverse y direction, p index. Correlations of the noise in the y direction are taken into account by the function C, which can be adapted to describe different physical scenarios, as we are going to illustrate in the context of ladder geometries in Sec. IV. Since the dW_t commute with one another, we have $C_{p_1,p_1',p_2,p_2'} = C_{p_2,p_2',p_1,p_1'}$. Hermiticity also imposes that $dW_t^{j,p,p'} = (dW_t^{j,p',p})^*$. Qualitatively speaking, each term in

the sum of Eq. (4) describes transitions from a state indexed by p' to a state indexed by p with a random complex amplitude given by $dW_t^{j,p,p'}$. Since the Cs are arbitrary, Eq. (4) constitutes the most general way of writing noisy quadratic jump processes between different transverse propagation modes. In one dimension, discussed in Sec. III, Eq. (4) reduces to an on-site stochastic fluctuation of potential, leading to standard dephasing, see also Eqs. (13) and (14). In Sec. IV, we will specify different noise-correlations on ladders and discuss their implication on transport.

The mean evolution generated by the stochastic Hamiltonian (4), with the prescription (5), is described by the Lindblad generator acting on the reduced density matrix of the system ρ,

$$\mathcal{L}(\rho) = \gamma \sum_{j,p_1,p_2,p_1',p_2'} C_{p_1,p_1',p_2,p_2'} \big(2a^\dagger_{j,p_1} a_{j,p_1'} \rho a^\dagger_{j,p_2} a_{j,p_2'} - \big\{a^\dagger_{j,p_2} a_{j,p_2'} a^\dagger_{j,p_1} a_{j,p_1'}, \rho\big\}\big) \tag{6}$$

where $\{,\}$ denotes anticommutation; see Appendix B.

A. Keldysh approach and exact self-consistent solution of transport in quantum stochastic resistors

As we will be dealing with systems under the effect of dephasing noise and biased leads, the dynamics of the system is intrinsically out of equilibrium. The natural language to describe these systems is the Keldysh formalism [51], detailed in Appendix A. The central objects of the theory are the retarded (R), advanced (A), and Keldysh (K) components of the single-particle Green's functions $\mathcal{G}^{R/A/K}$. They are defined in time representation as $\mathcal{G}^R_{j,m;i,n}(t-t') = -i\theta(t-t')\langle\{c_{j,m}(t), c^\dagger_{i,n}(t')\}\rangle$, $\mathcal{G}^A_{j,m;i,n}(t-t') = [\mathcal{G}^R_{i,n;j,m}(t'-t)]^*$ and $\mathcal{G}^K_{j,m;i,n}(t-t') = -i\langle[c_{j,m}(t), c^\dagger_{i,n}(t')]\rangle$ [52]. By adopting the notation by Larkin and Ovchinnikov [53], these three components are collected in a unique matrix, which obeys the Dyson equation

$$\boldsymbol{\mathcal{G}} = \begin{pmatrix} \mathcal{G}^R & \mathcal{G}^K \\ 0 & \mathcal{G}^A \end{pmatrix}, \quad \boldsymbol{\mathcal{G}}^{-1} = \boldsymbol{g}^{-1} - \boldsymbol{\Sigma}, \tag{7}$$

where $\boldsymbol{g}$ corresponds to the Green's function of the system disconnected from the leads and unaffected by noise. The matrix $\boldsymbol{\Sigma}$ corresponds to the self-energy, which has the same matrix structure as $\boldsymbol{\mathcal{G}}$.

In the path integral formalism, the fermionic degrees of freedom of the leads can be integrated out. Their integration gives a contribution to the self-energy of the system $\boldsymbol{\Sigma}_{\mathrm{L/R}}$, which has nonzero components only at the system edges $j = 1, N$. The general procedure of this integration is detailed in Appendix A. To give a more explicit idea of the result of this procedure, we report here the result for the simplest one-dimensional case ($M = 1$). The edge contributions then read in frequency space

$$\begin{aligned}
\Sigma^{R/A}_{\mathrm{L},i,j} &= t_x^2 g^{R/A}_{0,0} \delta_{i,j}\delta_{i,1}, \\
\Sigma^{R/A}_{\mathrm{R},i,j} &= t_x^2 g^{R/A}_{N+1,N+1} \delta_{i,j}\delta_{i,N}, \\
\Sigma^{K}_{\mathrm{L},i,j} &= 2it_x^2 F_{\mathrm{L}} \mathrm{Im}\big(g^R_{0,0}\big)\delta_{i,j}\delta_{i,1}, \\
\Sigma^{K}_{\mathrm{R},i,j} &= 2it_x^2 F_{\mathrm{R}} \mathrm{Im}\big(g^R_{N+1,N+1}\big)\delta_{i,j}\delta_{i,N},
\end{aligned} \tag{8}$$

where $\mathrm{Im}(\cdot)$ gives the imaginary part. The retarded and advanced components of the self-energy are renormalized by the corresponding reservoir Green functions, which are calculated at the site closest to the system. See Eq. (A7) for the explicit expression of $g^{R/A}_{0,0}(\omega)$ and $g^{R/A}_{N+1,N+1}(\omega)$ in the case of leads identical to the system. The Keldysh components describe the tendency of the edges of the system to equilibrate to the attached reservoirs. The functions $F_{\mathrm{L,R}}(\omega)$ describe the state of the leads, and the self-energies obey a local equilibrium fluctuation-dissipation relation [51]. In the absence of noise, the leads are considered in thermal equilibrium with a well-defined chemical potential $\mu_{\mathrm{L,R}}$ and shared temperature T. In frequency representation, this situation is described by $F_{\mathrm{L,R}}(\omega) = \tanh[(\omega - \mu_{\mathrm{L,R}})/2T]$. The fact that the system is out of equilibrium can be read in Eq. (8) via the fact that different functions F affect the self-energy of the system at its borders.

The Keldysh formulation of the problem is advantageous because it allows to deal exactly with the dephasing dynamics caused by the presence of the noise described by Eq. (4). Despite the quartic nature of Eq. (6), the stochastic formulation of the dephasing (4) allows for a closed exact solution of the self-energy [24,34,35]. Indeed, the latter can be expressed in terms of the Green's function via the relation

$$\boldsymbol{\Sigma}_\gamma(t,t')_{(j,p_1),(j',p_2')} = \gamma\delta(t-t')\delta_{j,j'} \sum_{p_1'p_2} C_{p_1,p_1',p_2,p_2'} \boldsymbol{\mathcal{G}}_{(j,p_1')(j,p_2)}(t,t), \tag{9}$$

which, inserted in Eq. (7), has to be solved self-consistently, see Appendix B. To summarize, we derive an explicit expression of the self-energies in the Dyson equation (7), which reads

$$\boldsymbol{\mathcal{G}}^{-1} = \boldsymbol{g}^{-1} - \boldsymbol{\Sigma}_{\mathrm{L}} - \boldsymbol{\Sigma}_{\mathrm{R}} - \boldsymbol{\Sigma}_\gamma\,, \tag{10}$$

where the expression of $\boldsymbol{\mathcal{G}}$ is obtained numerically.

Equipped with the formal expression of the single-particle Green's functions, we can directly and exactly inspect the transport properties of quantum systems under the influence of dephasing noise. By imposing a finite bias, $\mu_{\mathrm{L/R}} = \mu \pm \frac{\delta\mu}{2}$, between the right and left leads, a uniform longitudinal current J flows through the system. By construction, the noise (4) preserves the total density $n_{j,\mathrm{tot}} = \sum_p a^\dagger_{j,p} a_{j,p}$ at a fixed position j on the x axis, i.e., $[dH_t, n_{j,\mathrm{tot}}] = 0$. Thus, the definition of the total longitudinal current operator is unchanged by the noise term, and the current can be evaluated at any site j, namely

$$\begin{aligned}
J &= it_x \sum_{m=1}^{M} \langle c^\dagger_{j+1,m} c_{j,m} - c^\dagger_{j,m} c_{j+1,m}\rangle \\
&= t_x \sum_{m=1}^{M} \mathrm{Re}\big[G^K_{j,m;j+1,m}(t=0)\big]\,.
\end{aligned} \tag{11}$$

In the following, we will explicitly derive this expression from the exact self-consistent solution of Dyson's equation (9). Additionally, we rely on the linear expansion of Eq. (11) in the chemical potential difference $\delta\mu$ to study the conductance

of the system, which is defined as

$$G = \lim_{\delta\mu\to 0} 2\pi \frac{J}{\delta\mu}. \tag{12}$$

Notice that we rescaled the conductance by 2π in order to have the quantum of conductance equal to 1 and adopt the convention $e = k_B = \hbar = 1$. In the following sections, we devise a semiclassical model, which can capture the results from Eqs. (10), (11), and (12) in the presence of dephasing. In particular, we will inspect the conductance dependence on the chemical potential of the leads μ.

III. CONDUCTANCE OF A 1D QUANTUM STOCHASTIC RESISTOR

In this section, we focus on a strictly one-dimensional geometry to showcase the effectiveness of the semiclassical approach in describing the emergent diffusive transport properties of quantum stochastic resistors.

A. Exact derivation

We begin by deriving the dependence of the conductance G on the chemical potential of the leads μ, via the exact solution of a single chain subjected to on-site dephasing noise. In one dimension, the noise term in Eq. (4) reduces to

$$dH_t = \sqrt{2\gamma} \sum_j c_j^\dagger c_j dW_t^j, \tag{13}$$

with the corresponding Lindblad operator

$$\mathcal{L}(\rho) = \gamma \sum_j (2n_j \rho n_j - \{n_j, \rho\}). \tag{14}$$

For a QSH described by Eq. (4), the conductance of the system can be written

$$G_\gamma(\mu) = \int d\omega \frac{\mathcal{T}_\gamma(\omega)}{4T\cosh^2\left(\frac{\omega-\mu}{2T}\right)}. \tag{15}$$

Two equivalent expressions of $\mathcal{T}_\gamma(\omega)$ are derived in Appendix B, one relying on the expansion in $\delta\mu$ of Eq. (11), and the other on the expansion of the Meir-Wingreen formula as devised in Refs. [14,35]. The expression (15) for the conductance reproduces Landauer-Büttiker's formula, valid for noninteracting ballistic systems [54]. As such, $\mathcal{T}_\gamma(\omega)$ is interpreted as the transmittance of the channel at energy ω for a fixed γ, a quantity independent of the temperature T and chemical potential μ of the leads. An explicit expression of $\mathcal{T}_\gamma(\omega)$ was computed in Ref. [35] in similar settings. We stress that the extension of Landauer-Büttiker's formula (15) to dephased systems is highly nontrivial, given the fact that dephasing triggers inelastic scattering events in the conducting region.

If we consider leads, which are identical to the system, see Eq. (1), no reflection occurs at the interface and $\mathcal{T}_{\gamma=0}(\omega) = 1$ for $\omega \in [-2t_x, 2t_x]$ and 0 elsewhere. At zero temperature, this implies the usual quantized conductance $G = 1$ when the chemical potential of the leads lies within the dispersion relation of the reservoirs, $\mu \in [-2t_x, 2t_x]$ [1,55–57]; see Fig. 2.

The presence of any finite dephasing rate leads to diffusive transport in the thermodynamic limit [15,33–35,58]. In these

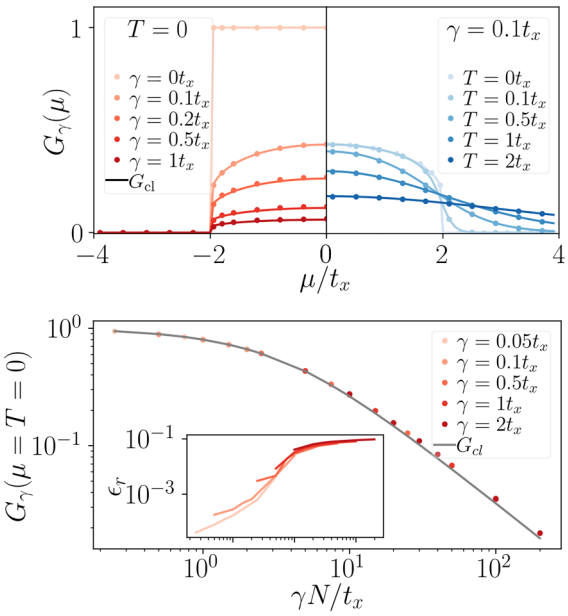

FIG. 2. (Top) Conductance as a function of chemical potential for increasing dephasing rates γ at $T = 0$ (left) and increasing temperature (right) at a fixed system size $N = 50$. The dots are derived relying on the exact quantum calculation (Sec. III A), while the dashed lines correspond to the semiclassical approximation (Sec. III B). (Bottom) Scaling of the conductance with the parameter γN when $T = 0$, $\mu = 0$. (Inset) Relative error of the semiclassical conductance at $\mu = 0$, $\epsilon_r = |G_{cl} - G_\gamma|/G_\gamma$.

studies, it was shown that the bulk transport properties are described by Fick's law

$$J = -D\nabla n, \tag{16}$$

where D is the diffusion constant and ∇n the particle density gradient along the chain. In particular, for fixed boundary conditions, Fick's law implies the $1/N$ suppression of the current with the system size and

$$D = \frac{2t_x^2}{\gamma}. \tag{17}$$

This suppression reveals the emergence of a resistive behavior, compatible with Ohm's law. This relation holds in the bulk *regardless* of the average chemical potential μ and temperature T of the biased leads. This fact can be understood as follows: at equilibrium, the effect of the noise term is to drive the system towards an infinite temperature state with a fixed number of particle [59]. Here the situation is more intricate since we are out-of-equilibrium. Nevertheless, we show numerically in Appendix D that, deep in the bulk, there exist a well-defined notion of *local equilibrium*, where the system does reach an infinite temperature state. Thus, in the bulk, the information about the energy scales of the leads is erased, and one expects that bulk transport properties, such as the diffusion constant, will be independent of the temperature and the chemical potentials of the boundaries. This point will be further emphasized in Sec. IV.

In contrast to the diffusion constant D, the conductance strongly depends on the temperature and chemical potential of the attached leads; see Fig. 2 (top) [60]. For a finite

dephasing rate γ, G_γ develops a clear dome-like dependence on the chemical potential [61] This shape persists even in the diffusive regime $N \gg t_x/\gamma$ where the conductance vanishes as $1/N$; see Fig. 2 (bottom) and Fig. 7 in Appendix C. At $T = 0$, the dome is restricted to energies within the bandwidth $[-2t_x, 2t_x]$ and the differential conductance $\partial_\mu G$ diverges whenever the chemical potential touches the edges of the band, even when $\gamma > 0$. This behavior is reminiscent of the "staircase" behavior of the conductance for noninteracting systems and $\gamma = 0$. The main difference is that for $\gamma > 0$ the conductance G is not quantized and acquires a μ dependence in the $[-2t_x, 2t_x]$ interval. As expected, increasing the temperature of the leads smears the dependence of the conductance with respect to the chemical potential, as illustrated in Fig. 2 (top).

The dome-like dependence of the conductance ultimately originates from its connection to the leads but it is independent of the microscopic details of the latter. Reservoirs with a linear band dispersion (i.e., not a cosine dispersion) would equally lead to a maximum of the conductance near the band center. Despite its usefulness, the numerical exact solution relies on relatively involved technical tools (Keldysh field theory and full diagrammatic ressummation), which somehow prevent a transparent interpretation of the phenomenology at work (e.g., the dome-shaped dependence of the conductance on μ). It is thus important to have a simpler description of transport that can simultaneously explain a constant diffusion constant, as well as the quantitative dependence of the conductance with the chemical potential.

In the next section, we show that a semiclassical model allows to build an intuitive physical explanation of the dependence of G_γ on the chemical potential and to connect it with the bulk behavior of transport.

B. Semiclassical approach

The Lindblad operator (14) can actually describe the average evolution of a system under different stochastic processes, which differ from the stochastic fluctuations of potential considered in Eq. (13). Indeed, the most natural way to devise a semiclassical description of the Lindblad dynamics of Eq. (14) is to "unravel" it to a projective measurement process, where the densities at each site are measured independently with rate γ [62,63]. Notice that for single realizations of the stochastic process, the projective dynamics fundamentally differs from the quantum stochastic dynamics described by Eq. (13). For instance, a density measurement on site j would project the system in a state with 1 or 0 particles on that site in a nonunitary fashion. On the contrary, the random potential fluctuations described by Eq. (13) are always unitary at the level of a single realization. Nevertheless, the projective and QSH dynamics coincide in average and are described by the same effective Lindblad operator (14).

In the projective case, at each time step Δt, a measurement at site j occurs with probability $\gamma \Delta t$. After a measurement, depending on whether the local particle number is measured to be zero or one, the density matrix is updated as follows:

$$\rho \to \rho_0 = \frac{(1-n_j)\rho(1-n_j)}{\mathrm{Tr}[\rho(1-n_j)]}, \quad \rho_1 = \frac{n_j \rho n_j}{\mathrm{Tr}[\rho n_j]}, \tag{18}$$

with respective probabilities

$$P_{\rho_0} = \mathrm{Tr}[\rho(1-n_j)], \quad P_{\rho_1} = \mathrm{Tr}[\rho n_j]. \tag{19}$$

Averaging over the possible outcomes for a small time step dt yields the average evolution of the density matrix $d\rho_t = \rho_{t+dt} - \rho_t$,

$$d\rho_t = \gamma dt \sum_j (2n_j \rho_t n_j - \{n_j, \rho\}), \tag{20}$$

which is equivalent to the Lindblad evolution described by Eq. (14).

This alternative point of view is the natural one to devise a semiclassical description of transport in systems affected by dephasing. If we consider a single-particle traveling through the chain, the effect of a measurement is to localize it at a given site j. When the particle is localized, it is in a superposition of all possible momentum states.

We thus propose the analogous classical model in the continuum limit: consider a single particle of initial velocity $v_0(\omega)$ coming from the left lead into the system of length $\ell = Na$, where a is the lattice spacing. Its velocity is set by its energy ω, $v_0(\omega) = \partial \epsilon_k / \partial k|_\omega$, where ϵ_k is the dispersion relation of the lead, see Fig. 1 (bottom). At a random time t, determined by the Poissonian probability distribution $p(t) = \gamma e^{-\gamma t}$, its velocity is reinitialized by drawing a momentum k sampled from a uniform probability distribution on the interval $[-\pi, \pi]$. For a dispersion relation $\epsilon_k = -2t_x \cos(k)$, the probability distribution of the velocity v reads

$$p(v) = \frac{1}{2\pi t_x \sqrt{1 - \left(\frac{v}{2t_x}\right)^2}}, \quad v \in [-2t_x, 2t_x]. \tag{21}$$

Once the velocity has been reset, the process is restarted. Whenever the particle reaches one boundary located at $x = 0$ or $x = \ell$, it exits the system. The problem of computing the semiclassical transmittance $\mathcal{T}_{\mathrm{cl}}$ can be reduced to compute the probability of exiting the system by touching the right boundary. Note that this problem differs from a usual random walk, as in this case the length of the steps are not uniform in time.

Once a measurement occurs, the velocity of a particle injected by a reservoir gets totally randomized according to the probability distribution (21). Thus the object of interest becomes the probability $P(x)$ of exiting the system once a given measurement has taken place at some position $x \in [0, \ell]$. The first measurement takes place at position x and time $t = x/v_0(\omega)$ with Poissonian probability distribution $\gamma e^{-\gamma t}$. Thus, the semiclassical transmittance $\mathcal{T}_{\mathrm{cl}}$, for a particle injected from the left lead with velocity $v_0(\omega)$, is given by

$$\mathcal{T}_{\mathrm{cl}}(\omega) = \int_0^\infty P(x) \frac{\gamma}{v_0(\omega)} e^{-\gamma \frac{x}{v_0(\omega)}} dx\,. \tag{22}$$

We recall that, because of the specific dispersion of the leads under consideration, $\mathcal{T}_{\mathrm{cl}}(|\omega| > 2t_x) = 0$.

It remains to determine $P(x)$. It is useful to introduce the probability $P_v(x)$ for a particle to exit on the right when it starts at x with velocity v. The probability $P(x)$ is thus the integral of this probability over all possible velocities, $P(x) = \int dv\, p(v) P_v(x)$. As we assume that no measurement process

occurs in the leads, $P(x)$ has to fulfill the boundary conditions

$$P(x<0)=0, \quad P(x>\ell)=1. \tag{23}$$

In the system, where the measurement processes occur, $P_v(x)$ is expressed in the closed form

$$P_v(x)=\theta(v)\left[e^{-\gamma\frac{\ell-x}{v}}+\int_0^{\frac{\ell-x}{v}} dt\gamma e^{-\gamma t}P(x+vt)\right] + \theta(-v)\int_0^{-\frac{x}{v}} dt\,\gamma e^{-\gamma t}P(x+vt) \tag{24}$$

where $\theta(v)$ is the usual Heaviside step function. The first term corresponds to the probability that the particle goes through the system without the occurrence of any measurement. The second term is the probability that a right mover resets at time t multiplied by the probability to exit if the particle starts again from this position. The last term corresponds to the same process but for a left mover. By integrating over the distribution of velocities (21), we get an implicit equation for $P(x)$ for $x\in[0,\ell]$,

$$P(x)=\varphi(\ell-x)-\int_0^{\ell-x} dy\,\varphi'(y)\,P(x+y) - \int_0^{x} dy\,\varphi'(y)\,P(x-y) \tag{25}$$

where we have introduced the function

$$\varphi(y)=\int_0^{\infty} dv\,p(v)\,e^{-\gamma\frac{y}{v}}=\int_0^1 dx\,\frac{e^{-\frac{\gamma y}{2t_x x}}}{\pi\sqrt{1-x^2}}, \tag{26}$$

and $\varphi'(y)=\partial\varphi/\partial y$. From Eq. (25), the probability $P(x)$ can be in principle derived iteratively in the number of measurement-induced resets of velocity. This solution would consist in writing

$$P(x)=\sum_{n=0}^{\infty}P_n(x), \tag{27}$$

where $P_n(x)$ is the probability of exiting on the left after n resets starting from x. This leads to

$$P_0(x)=\varphi(\ell-x), \tag{28}$$

$$P_{n+1}(x)=-\int_0^{\ell-x} dy\,\varphi'(y)\,P_n(x+y) - \int_0^{x} dy\,\varphi'(y)\,P_n(x-y). \tag{29}$$

Nevertheless, we have found empirically that solving Eq. (25) self-consistently provides faster convergence and numerical stability [64] in comparison to the recursive solution (27). We use the derived solution in Eq. (22), to obtain the semiclassical expression of the transmittance.

Using the newly found transmittance in formula (15), we compute the associated semiclassical conductance $G_{\rm cl}$. In Fig. 2, we compare $G_{\rm cl}$ (solid lines) with the exact quantum calculation G_γ (dots) and find an excellent agreement for all chemical potentials and temperatures.

Deep in the diffusive region, $N\gg t_x/\gamma$, the semiclassical model has some deviations with respect to the quantum solution. In the inset of Fig. 2 (bottom), we depict the relative error $\epsilon_r=|G_{cl}-G_\gamma|/G_\gamma$ in the middle of the spectrum and verify it does not increase above 10%. One possible explanation for this discrepancy could be that the semiclassical model assumes that at each reset event the new momentum is drawn uniformly in the interval $[-\pi,\pi]$ and the particle has ballistic propagation at the corresponding velocity. In principle, we have to take into account the mode occupation of the fermions in the system. Indeed, the exclusion principle should prevent the particle to acquire a momentum corresponding to an already occupied mode. Taking these effects into account is, however, beyond the scope of this paper. We also stress that within this approach, we have considered leads and systems described by the same Hamiltonian in absence of dephasing. This assumption ensures that we do not need to take into account any additional reflection phenomena that might occur when the particle is transferred from the leads to the system.

The semiclassical picture provides an intuitive explanation of the conductance drop observed close to the band edges, $\mu_{\rm edge}=\pm 2t_x$. Close to these points, the velocity of incoming particles is the lowest. It is then more likely that a measurement process will occur and reset its speed, increasing its chance to backscatter into the original lead, and thus reducing the conductance. Additionally, the first measurement process resets the single-particle velocity, leading to a uniform distribution of the particle over all the accessible states. Thus, after the measurement the particle attains an infinite temperature state, which is reservoir-independent and is the one related to the bulk transport properties described by the diffusion constant (17). Remark that this picture is consistent with the fact that the diffusion constant evaluated in the bulk is independent of the boundary chemical potentials and temperatures. In conclusion, this simple semiclassical physical picture connects bulk and boundary effects on the transport properties of this system, which are revealed by the diffusion constant and the conductance respectively.

IV. DEPHASED LADDER

We now extend the result for the conductivity of a 1D system to a ladder made of M legs in the transverse direction, as described by the Hamiltonian (1), see also Fig. 1. In this section, we consider noises that are site-to-site independent along the x axis, but without a fixed structure in the y direction. Even though a natural choice is to consider noise processes, which are uncorrelated along the y direction (as we will do), considering also correlated structures is motivated from synthetic dimensions setups. These setups make use of coupling between nonspatial degrees of freedom to simulate motion along additional dimensions [46–49]. In our setup, the x direction would correspond to the physical dimension while the synthetic dimension is mapped to the transverse y direction. With this mapping, the QSH studied here could be realized from randomly oscillating potentials that are spatially resolved in the physical direction; see also Sec. V.

We recall the generic expression for the QSH Eq. (4),

$$dH_t=\sqrt{2\gamma}\sum_{j,p,p'}a^\dagger_{j,p}a_{j,p'}dW_t^{j,p,p'}, \tag{30}$$

with the covariance of the noise $dW_t^{j_1,p_1,p_1'} dW_t^{j_2,p_2,p_2'} = \delta_{j_1,j_2} C_{p_1,p_1',p_2,p_2'} dt$. Each term of the sum describes a transition from a state indexed by p' to a state indexed by p with a random complex amplitude given by $dW_t^{j,p,p'}$. It is the most general way of writing noisy quadratic jump processes between different states in the y direction.

In what follows, we will investigate the transport for different geometries of the noise by specifying the covariance tensor C.

A. Noise I

We start with the simplest case, that we label Noise I. It involves a single uniform noise acting on a given vertical section of the system, see also Fig. 1 (top). It is described by

$$C^{\mathrm{I}}_{p_1,p_2,p_1',p_2'} = \delta_{p_1,p_2}\delta_{p_2,p_1'}\delta_{p_1',p_2'}\,, \tag{31}$$

which corresponds to a QSH of the form

$$dH_t^{\mathrm{I}} = \sqrt{2\gamma}\sum_{j,m} c^\dagger_{j,m} c_{j,m} dB_t^j = \sqrt{2\gamma}\sum_{j,p} a^\dagger_{j,p} a_{j,p} dB_t^j\,, \tag{32}$$

with $\{B_t^j\}$ independent Brownian processes (recall that m indexes the spatial degrees of freedom in the y direction while p indexes the transverse modes). This kind of noise can be naturally implemented in synthetic ladders generated from internal spin degrees of freedoms of ultracold atoms [46–49]. Equation (31) would correspond to a randomly fluctuating potential that acts independently on each atom and uniformly shifts the energy levels of each spin state by $\sqrt{2\gamma}$.

The noise dH_t^{I} commutes at fixed j with the occupation number operator of every mode p, $a^\dagger_{j,p} a_{j,p}$, and therefore does not couple different modes. As a consequence, all the results that we have derived for the conductance of a 1D system can be trivially extended to the present case since the system is then equivalent to a collection of uncoupled 1D bands. The dispersion associated to each band $\epsilon_p(k)$ is the same than for the 1D case with an overall energy shift given by $\epsilon_p(\pi/2)$. Thus, the total conductance is the sum of the contribution of each mode, namely,

$$G_{\mathrm{I}}(\mu) = \sum_p G_\gamma\Big[\mu - \epsilon_p\Big(\frac{\pi}{2}\Big)\Big]\,, \tag{33}$$

where G_γ is given by Eq. (15), extensively studied in the purely 1D case.

In the absence of dephasing and at zero temperature ($\gamma = T = 0$), the conductance shows the usual staircase quantization with respect to the chemical potential. As it is shown in Fig. 3 for a two-leg ladder, the jumps in conductance take place whenever the number of bands crossed by the chemical potential changes. For a finite rate γ, the action of the dephasing noise is the same for each individual band and, as a consequence, the total conductance decays as $1/N$ for larger systems.

We stress that since Noise I does not mix the different modes, it cannot change the value of their occupation number, which is set by the chemical potential in the reservoirs. For instance, if a given mode was initially empty, it will remain so in the steady state. However, at fixed p, within *a single band*, the dephasing noise (13) drives the density matrix to a state proportional to the identity [59], which is reminiscent of the infinite temperature state discussed in the 1D case, see also Appendix D. We therefore say that Noise I is *maximally mixing* the modes k in the x direction but not mixing at all the modes p in the y direction. As a consequence, it does not drive the system to a genuine infinite temperature state, this only happens within each individual band. A picture of this stationary state for increasing chemical potentials is sketched in Fig. 3.

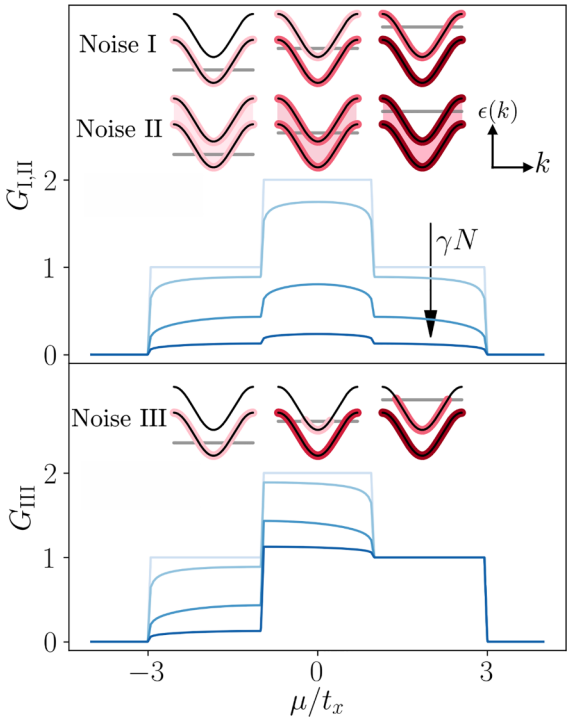

FIG. 3. Conductance profiles for different correlations of the noise (30) and increasing values of γN. For increasing shades of blue: $\gamma = 0$; $\gamma = 0.1\,t_x, N = 5$; $\gamma = 0.5\,t_x, N = 10$ and $\gamma = 0.5\,t_x, N = 50$ and $t_y = t_x$. Noise I and II share the same conductance profile, while Noise III features the coexistence of ballistic and diffusive transport, see main text. The sketches on top of the conductance plots depict the stationary state reached in the bulk. These states may or may not depend on the position of the chemical potential μ in the reservoirs (horizontal-grey lines), with respect to the dispersion relations of the different conduction modes in the system (black lines). The red halo on top of the dispersion relations indicates the occupation probability of the modes. Noise I distributes particle uniformly within each band separately, while Noise II distributes the states in all bands isotropically. Noise III is a special case, which preserves the shape of the zero temperature distribution of the reservoirs in the bulk only in the upper band.

We now show that the conductance profile illustrated in Fig. 3 is not unique to the uncorrelated Noise I (31), and also describes other types of geometries.

B. Noise II

In this section, we consider an isotropic case, where the noise is uncorrelated both in the x and y directions. In this

case, that we label Noise II, the QSH in position basis reads

$$dH_t^{\mathrm{II}} = \sqrt{2\gamma}\sum_{j,m} c_{j,m}^\dagger c_{j,m} dB_t^{j,m}\,, \tag{34}$$

with $dB_t^{j_1,m_1} dB_t^{j_2,m_2} = \delta_{j_1,j_2}\delta_{m_1,m_2} dt$. After performing the unitary transformation that diagonalizes the nonstochastic problem (1) in the form (2), we find the noise correlation function

$$C^{\mathrm{II}}_{\substack{p_1,p_1',\\ p_2,p_2'}} = \left(\frac{2}{M+1}\right)^2 \sum_{m=1}^{M} \prod_{\substack{a=p_1,\\ p_1',p_2,p_2'}} \sin\left(\frac{\pi a m}{M+1}\right). \tag{35}$$

Contrary to the previous case, Noise II is maximally mixing for the modes k in the x direction and for the modes p in the y direction. As a consequence, this noise drives the system to a genuine infinite temperature state in the bulk; see also sketches in Fig. 3. The mixing of the modes in the transverse direction renders the task of computing the conductance an *a priori* nontrivial one.

Nevertheless, as we show in Appendix E, for any noise satisfying the condition

$$\sum_p C_{p_1,p,p,p_2} = \mathcal{N}\delta_{p_1,p_2}\,, \tag{36}$$

the equations of motion of the total current J coincide to those generated by Noise I up to a renormalization of γ by a constant $\mathcal{N}$. As shown in the Appendix E, this condition corresponds $\forall p$ to $(a_{j,p}^\dagger, a_{j,p})$ being eigenvectors of the dual Lindbladian $\mathcal{L}^*$ with the same eigenvalue $\mathcal{N}$. The fact that $\mathcal{L}^*$ act the same way on the transverse modes can be seen as an isotropy condition for the noise term, i.e., this term cannot discriminate between longitudinal modes and hence, cannot change the value of the total current.

Using that $\delta_{a,a'} = \frac{2}{M+1}\sum_j \sin(\frac{\pi a j}{M+1})\sin(\frac{\pi a' j}{M+1})$, one can verify that C^{II} satisfies condition (36) with $\mathcal{N} = 1$. Thus we find that

$$G_{\mathrm{I}}(\mu) = G_{\mathrm{II}}(\mu)\,. \tag{37}$$

This result may sound surprising as, even though Noise II drives the system towards the maximally mixed, infinite temperature state, the staircase behavior of G is preserved, i.e., there is a discontinuity of $\partial_\mu G$ every time the chemical potential touches a band.

The remarkable equality (37) can be intuitively understood within the semiclassical picture. All that matters for the conductance is the number of modes that can contribute to the current. This number is fixed by the chemical potential, which in turn controls the staircase behavior of the conductance. Once a particle has entered the system, different scattering events may switch it from one channel to the other isotropically, as expressed mathematically by the condition (36). Nevertheless, all the channels carry the current in the same fashion, since the dispersion relations of all the transverse modes coincide in quasi-momentum k, except for an irrelevant energy shift. As a consequence, the total conductance is insensitive to whether the noise is coherent (or not) along the transverse direction.

C. Noise III

Finally, we illustrate how breaking the condition (36) may lead to exotic transport. We introduce the case of Noise III, where the correlations C^{III} of Noise III are designed such that they only couple pairs of transverse modes,

$$C^{\mathrm{III}}_{p_1,p_1',p_2,p_2'} = f_{p_1,p_2}\delta_{p_1,p_2'}\delta_{p_1',p_2}\,, \tag{38}$$

for which

$$\sum_p C^{\mathrm{III}}_{p_1,p,p,p_2} = \delta_{p_1 p_2}\sum_p f_{p_1,p}\,. \tag{39}$$

This qualitatively corresponds to the case where, for any noisy process that transfers a particle from the band p_1 to p_2, there is the reverse process that transfers a particle from p_2 to p_1 with the same rate f_{p_1,p_2}.

The isotropy condition (36) is fulfilled if, for example, we impose f_{p_1,p_2} to be equal to a constant c for every (p_1, p_2) in which case we have that $\mathcal{N} = Mc$.

Breaking the isotropy condition can lead to a hybrid type of transport. For instance, let us consider the case where

$$f_{p_1,p_2} = \delta_{p_1,p_2}\theta(p - p_0)\,, \tag{40}$$

with the convention $\theta(0) = 0$ for the Heaviside step function. This noise imposes diffusive transport to the lowest transverse modes ($p \leqslant p_0$) while the highest modes ($p > p_0$) remain ballistic. Since this noise does not couple the different transverse modes, the conductance has both ballistic and diffusive contributions,

$$G_{\mathrm{III}}(\mu) = \sum_{p\leqslant p_0} G_\gamma(\mu - \epsilon_{y,p}) + \sum_{p>p_0} G_{\gamma=0}(\mu - \epsilon_{y,p}). \tag{41}$$

We plot an example of such situation on Fig. 3 (bottom) for a two-leg ladder and $p_0 = 1$. The overall current has diffusive behavior until the chemical potential reaches the bottom of the upper band at $\mu_0 = -2t_x - 2t_y\cos(\frac{p_0\pi}{M+1})$. For $\mu \geqslant \mu_0$ the ballistic mode starts contributing and dominates the conductance in the thermodynamic limit $N \to \infty$

V. CONCLUSIONS AND PERSPECTIVES

In this paper, we have studied the current flowing through M-leg ladders subject to external dephasing noises with different correlations along the direction y transverse to transport. Starting from the purely one-dimensional case, $M = 1$, we have devised a semiclassical model to compute the conductance as a function of the chemical potential and found excellent agreement with numerical solutions obtained from exact self-consistent calculations of Dyson's equation.

Showing the effectiveness of this semiclassical model is important as it allows to build a simple and intuitive physical picture of the emergence of bulk resistive behavior in quantum stochastic resistors. As extensively discussed in the core of this paper, the bulk transport properties of these systems, such as the diffusion constant or the resistivity, are insensitive to the temperature and chemical potential of the connected reservoirs. We showed that this is not the case for their conductance and that we could rely on the semiclassical approach to bridge between boundary and bulk effects. It could be interesting to understand the deeper connections between our semiclassical

model and the quasiparticle picture recently introduced to describe entanglement growth [65,66].

The effectiveness of the semiclassical approach may also hint to a potential connection to Drude models of impurity scattering. As in Drude models, the dependence of the conductance on the chemical potential shown in Fig. 2 is somehow directly related to the inverse of the density of states of the system. Even though the semiclassical approach in our case strongly relies on the unraveling of the Lindblad operator to a measurement process, we can also understand the local dephasing as induced by a local phonon bath at infinite temperature. Whether such unraveling is possible/relevant for more generic scattering problems, also in higher dimensions, remains to be understood.

We have also shown that these nontrivial results in one dimension could be also extended to M-leg ladder systems. In particular, we have shown that the results valid in 1D could be immediately applied to the case where the noise term preserves the coherence in the vertical direction, this case being particularly relevant to systems featuring synthetic dimensions [46–49]. In this case, the total conductance is just the sum of the contributions of independent 1D channels and its diffusion constant remains unchanged.

We then demonstrated that the coherence properties of the noise along the y direction do not play a role on the conductance of a ladder system when the noise fulfills the condition (36). We also showed that breaking this condition for the correlations of the noise allows to engineer exotic transport. We gave an example (Noise III) where the longitudinal current switches between a diffusive or ballistic behavior depending on the chemical potential.

The isotropy condition (36) can be understood as the condition under which each transverse mode contributes to the total longitudinal current in the same manner. This raises the natural question of understanding what would happen if this degeneracy were to be lifted. A particularly interesting problem would be to understand the effect of density-density interactions in the transverse direction to the transport. In the two-leg ladder, numerical studies relying on DMRG techniques could be supported by the infinite system size perturbation technique recently introduced in Ref. [35].

We briefly comment on the prospect of experimental realizations. The noise discussed here is specially suitable for implementation in synthetic dimensions setups such as ultracold atoms in shaken constricted optical channels [67] or with synthetic spin dimension [46–49,68], or even photonic systems with ring resonator arrays [69,70]. In these systems, the synthetic dimension plays the role of transverse direction in our model while the physical dimension encodes the longitudinal direction. A dephasing noise in the physical dimension would thus affect in the same manner all the synthetic sites, giving a natural realization of Noise I described by Eq. (31).

ACKNOWLEDGMENTS

The authors thank Iacopo Carusotto for helpful discussions. This work has been supported by the Swiss National Science Foundation under Division II. J.S.F. and M.F. acknowledge support from the FNS/SNF Ambizione Grant No. PZ00P2_174038.

APPENDIX A: GREEN'S FUNCTION OF THE FREE SYSTEM

To compute the current operator (11), one first needs to compute the Green's function of the lead alone and of the system in presence of the leads. For simplicity, we treat here the 1D channel but generalization to M legs will be straightforward. For a single left lead, the Hamiltonian (1) can be divided as

$$H = H_{\mathrm{S}} + H_{\mathrm{L}} - t_x(c_0^\dagger c_1 + c_1^\dagger c_0). \tag{A1}$$

We suppose the lead (L) and the system (S) to be noninteracting so that $H_{\mathrm{L,S}}$ is a quadratic Hamiltonian. The associated action in the Keldysh formalism, using Larkin notation [53] for the fermionic fields,

$$\begin{aligned} S = S_{\mathrm{S}} + \int \frac{d\omega}{2\pi}([\bar\psi_{\mathrm{L}}]\boldsymbol{g}_{\mathrm{L}}^{-1}[\psi_{\mathrm{L}}]) \\ + t_x\left(\bar\psi_0^1\psi_1^1 + \bar\psi_0^2\psi_1^2 + \bar\psi_1^1\psi_0^1 + \bar\psi_1^2\psi_0^2\right) \end{aligned} \tag{A2}$$

where S_{S} is the action of the system, $[\psi_{\mathrm{L}}]$ is a vector containing all Grassman variables associated to the left lead and $\boldsymbol{g}$ is the Green's function before coupling, with the same matrix structure as $\boldsymbol{\mathcal{G}}$ in Eq. (7), $\boldsymbol{g} := \left(\begin{smallmatrix} g^R & g^K \\ 0 & g^A \end{smallmatrix}\right)$. Integrating out the lead's degrees of freedom, one finds

$$\begin{aligned} S &= S_{\mathrm{S}} - \int \frac{d\omega}{2\pi}\begin{pmatrix}\bar\psi_1^1 & \bar\psi_1^2\end{pmatrix}\begin{pmatrix}\Sigma^R & \Sigma^K \\ 0 & \Sigma^A\end{pmatrix}\begin{pmatrix}\psi_1^1 \\ \psi_1^2\end{pmatrix}, \\ \Sigma^{R/A/K} &= t_x^2 g_{0,0}^{R/A/K}. \end{aligned} \tag{A3}$$

For an infinite-size lead made of n discrete sites with a tight-binding Hamiltonian coinciding with Eq. (1), the spectrum is given by $\epsilon_k = -2t_x\cos(\frac{k\pi}{n+1})$, $k \in [1, n]$. The associated retarded Green's function in momentum space is given by (the tilde designates momentum space)

$$\tilde g_{k,k'}^R(\omega) = \frac{\delta_{k,k'}}{\omega + 2t_x\cos\left(\frac{k\pi}{n+1}\right) + i0^+}. \tag{A4}$$

In position space, this yields

$$\begin{aligned} g_{j,j'}^R = \frac{2}{n+1}\sum_k \sin\left(\frac{k(j+1)\pi}{n+1}\right)\sin\left(\frac{k(j'+1)\pi}{n+1}\right) \\ \times \frac{1}{\omega + 2t_x\cos\left(\frac{k\pi}{n+1}\right) + i0^+}. \end{aligned} \tag{A5}$$

We are interested in the $j = j' = 0$ term in the semi-infinite limit, i.e., we take $n \to \infty$. Introducing $p = \frac{k\pi}{n+1}$, we get

$$g_{0,0}^R = \frac{2}{\pi}\int_0^\pi dp \frac{\sin^2 p}{(\omega + 2t_x\cos p + i0^+)}, \tag{A6}$$

which can be computed by contour integral in the complex plane to be

$$g_{0,0}^R = \frac{1}{2t_x^2}(\omega + i0^+ - i\sqrt{(2t_x)^2 - (\omega + i0^+)^2}). \tag{A7}$$

The advanced component is just the complex conjugate of the retarded one. To obtain the Keldysh component, we will

suppose that the lead is at thermal equilibrium so that

$$g^K_{0,0}(\omega) = \tanh\left(\frac{\omega-\mu}{2T}\right) 2i\mathrm{Im}\big(g^R_{0,0}\big) = -\theta(2t_x - |\omega|)\frac{i}{t_x^2}\tanh\left(\frac{\omega-\mu}{2T}\right)\sqrt{(2t_x)^2-\omega^2}\,, \tag{A8}$$

which is enough to compute the Green's function of the system in presence of the leads [71]. In the absence of noise, the Green's function of the system is easily computed by noticing that the system with both leads constitutes a discrete tight-binding chain of infinite size. In this case, the Green's function in momentum space is given by

$$\tilde{\mathcal{G}}^R(p,p') = \frac{\delta(p-p')}{\omega + 2t_x\cos p + i0^+}. \tag{A9}$$

By doing the inverse Fourier transform we get it in position space

$$\mathcal{G}^R_{j,k} = \int_{-\pi}^{\pi}\frac{dp}{2\pi}\frac{e^{-ip(j-k)}}{\omega + 2t_x\cos p + i0^+}\,, \tag{A10}$$

which can be again computed by contour integral to be

$$\mathcal{G}^R_{j,k} = \frac{z_+^{k-j}}{t_x(z_+ - z_-)}\,, \tag{A11}$$

for $j \leqslant k$ with $z_\pm = -(\frac{\omega+i0^+}{2t_x}) \pm i\sqrt{1-(\frac{\omega+i0^+}{2t_x})^2}$. Using the symmetry property $\mathcal{G}^R_{j,k} = \mathcal{G}^R_{k,j}$ we have the full Green's function in position space.

APPENDIX B: DERIVATION OF THE EXACT SELF-CONSISTENT EQUATION AND OF THE TRANSMITTANCE OF QUANTUM STOCHASTIC RESISTORS

In this section, we summarize the derivation of the self-consistent condition (9) as obtained in previous papers [24,35]. We also explain the factorization of the current in the form of Eq. (15). We also derive the Linbdlad equation describing the dynamics of QHS averaged over the noise realizations.

1. Self-consistent equation

In full generality and to improve readability, we consider a more compact formulation of the noise than in Eq. (4), where $dH_t = \sum_{i,j}\sqrt{2\gamma}c_i^\dagger c_j dW_t^{i,j}$ and i, j are indices labeling generic lattice sites on an arbitrary lattice and $dW_t^{i,j}dW_{t'}^{k,l} = C_{ijkl}dt$ when $t = t'$ and 0 elsewhere.

The action associated to this noise reads

$$S_\gamma = -\sum_{i,j}\int\sqrt{2\gamma}\big(\bar\psi^1_{i,t}\psi^1_{j,t} + \bar\psi^2_{i,t}\psi^2_{j,t}\big)dW_t^{i,j}\,. \tag{B1}$$

We consider the diagrammatic representation of the Green's function in Fig. 4. Full lines represent the retarded propagator, dashed lines the advanced one and mixed lines the Keldysh propagator. We represent with wiggly lines the two vertex associated to the noise action (B1), one connecting only solid lines and the other only dashed ones. The first contributions

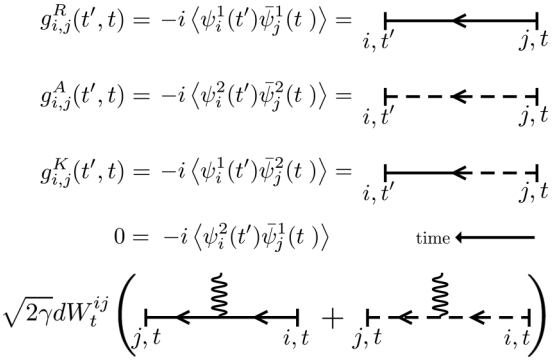

FIG. 4. Diagrammatic representation of the retarded (R), advanced (A), and Keldysh (K) Green's function. Time flows from right to left. On the bottom, we add the diagrammatic representation of the vertex provided by the action (B1), which preserves dashed and solid lines.

to the diagrams of $\mathcal{G}^{R,A,K}$ are depicted in Fig. 5. One readily realizes that in the diagrammatic expansion of the retarded (advanced) propagators only retarded (advanced) propagators appear. For the Keldysh component, one can switch only once from dashed to solid lines through the insertion of a Keldysh propagator.

The average over different noise realizations is computed using the Itō rules, which impose an equal time index when connecting wiggly lines, $dW_t dW_{t'} \neq 0 \Rightarrow t' = t$. Diagrammatically, wiggly lines merge as shown in Fig. 6. The key insight is that after noise-averaging the diagrams, those with crossing wiggly lines do not contribute to the action. In Fig. 5, we show a diagram with crossing wiggly lines arising from the diagrammatic expansion of the Keldysh component. In that example, after averaging, two retarded propagators (labeled A and B) have opposite directions. In our representation, this implies the multiplication of two retarded functions with opposite time dependence, which equals 0. Similar considerations apply for all crossing diagrams, and we direct the interested reader to Refs. [24,35] for the complete demonstration. Since the crossing diagrams vanish, the Born noncrossing approximation is exact, and all the remaining rainbow diagrams can be exactly resummed, leading to the

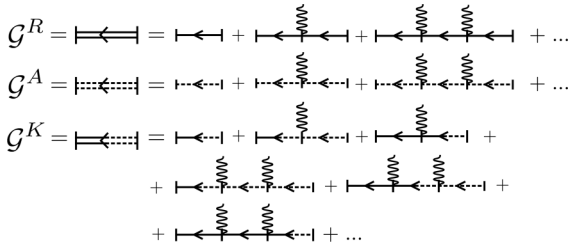

FIG. 5. Diagrammatic expansion of the retarded, advanced, and Keldysh propagators in the quantum stochastic action (B1). At a given order n in the expansion, the retarded/advanced component of the self energy only has one diagram whereas the Keldysh component has $n+1$ diagrams, corresponding to the insertion of the Keldysh bare component at different times.

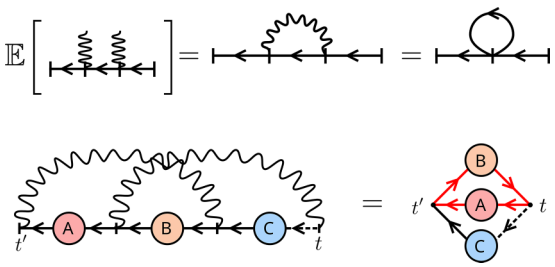

FIG. 6. Example of a crossing diagram for the Keldysh component. The red lines highlight the part of the diagram violating the causality structure and are responsible for making the diagram vanish.

following self-consistent equation for the self-energy

$$\mathbf{\Sigma}_{\gamma,ij}(t,t') = \gamma\delta(t-t')\sum_{kl} C_{iklj}\boldsymbol{\mathcal{G}}_{kl}(t,t)\,, \tag{B2}$$

which is equivalent to Eq. (9) in the main text.

2. Transmittance of a quantum stochastic resistor

We derive now two explicit and equivalent expressions of the transmittance $\mathcal{T}_\gamma(\omega)$ used to derive the conductance in Eq. (15). To do this, we rely first on the Meir-Wingreen expression of the current flowing from the reservoirs to the system [14,72],

$$J = \frac{i}{2}\int\frac{d\omega}{2\pi}\mathrm{Tr}\{[\Gamma_\mathrm{L}(\omega)-\Gamma_\mathrm{R}(\omega)]\mathcal{G}^K(\omega) - [F_\mathrm{L}(\omega)\Gamma_\mathrm{L}(\omega)-F_\mathrm{R}(\omega)\Gamma_\mathrm{R}(\omega)][\mathcal{G}^R(\omega)-\mathcal{G}^A(\omega)]\}\,, \tag{B3}$$

where the trace is performed over spatial indices, $F_{\mathrm{L/R}}(\omega) = \tanh[\beta(\omega-\mu_{\mathrm{L/R}})/2]$ gives the equilibrium state of the right (R) and left (L) reservoirs, and $\Gamma_{\mathrm{L/R}}(\omega) = -\mathrm{Im}(\Sigma_{\mathrm{L/R}})/\pi$ are the frequency-dependent hybridization functions describing the coupling of the system with its left and right reservoirs. In the idealized case of Sec. III, where system and reservoirs are identical, the explicit expression of these hybridization functions can be derived from Eq. (8) and (A7), so that $\Gamma_{i,j;\mathrm{L/R}}(\omega) = \delta_{i,j}\delta_{i,1/N}\Gamma(\omega)$ in the interval $\omega\in[-2t_x,2t_x]$, with $\Gamma(\omega) = (\sqrt{4t_x^2-\omega^2})/2\pi$. Outside of the interval $\omega\in[-2t_x,2t_x]$, $\Gamma(\omega)=0$. Remind that we take $j=1$ and N as the leftmost and rightmost sites of the one-dimensional system.

We focus on the case of identical reservoirs exchanging particles with the system only at one site and that the Meir-Wingreen formula (B3) thus simplifies to

$$J = \int d\omega\Gamma(\omega)\left[\frac{i}{2}\frac{\mathcal{G}_1^K(\omega)-\mathcal{G}_N^K(\omega)}{2\pi} + \frac{F_\mathrm{R}(\omega)-F_\mathrm{L}(\omega)}{2}\mathcal{A}(\omega)\right], \tag{B4}$$

where we have introduced the shorthand notation $\mathcal{G}_i^{R/A/K} = \mathcal{G}_{ii}^{R/A/K}$ and assumed a mirror symmetric system, so that the spectral functions at the system edges, $\mathcal{A}(\omega) = \mathcal{A}_{1/N}(\omega) = -\mathrm{Im}[\mathcal{G}_{1/N}^R(\omega)]/\pi$, is the same at both edges. The above expression requires the derivation of the Keldysh Green's functions $\mathcal{G}_i^K(\omega)$, which are derived by solving the self-consistent equation

$$\mathcal{G}_{ij}^K(\omega) = -\mathcal{G}_{il}^R(\omega)\left[g^{-1,K}(\omega)-\Sigma_\gamma^K(\omega)\right]_{lm}\mathcal{G}_{mj}^A(\omega)\,, \tag{B5}$$

where we use the convention of the summation of repeated indices and where Σ_γ^K is given by the Keldysh component of Eq. (B2).

For the specific case of the on-site dephasing of Sec. III, $C_{ijkl} = \delta_{ij}\delta_{ik}\delta_{kl}$ and the self-consistent equation (B2) can be cast in the form

$$[\delta_{ij}-M_{ij}]\mathcal{G}_j^K(t,t) = D_i, \tag{B6}$$

where we have introduced the matrix and vector notations

$$M_{ij} = \gamma\int\frac{d\omega}{2\pi}\mathcal{M}_{ij}(\omega), \quad \mathcal{M}_{ij}(\omega) = \left|\mathcal{G}_{ij}^R(\omega)\right|^2, \tag{B7}$$

$$D_{ij} = -\int\frac{d\omega}{2\pi}\mathcal{G}_{ij}^R(\omega)g_{jk}^{-1,K}(\omega)\mathcal{G}_{kj}^A(\omega), \quad D_i = D_{ii}\,, \tag{B8}$$

where we also exploited the property $\mathcal{G}_{ij}^A(\omega) = [\mathcal{G}_{ji}^R(\omega)]^*$. Generalized forms of Eqs. (A3) and (A8) lead to

$$g^{-1K}(\omega) = 2\pi i[F_\mathrm{L}(\omega)\Gamma_\mathrm{L}(\omega)+F_\mathrm{R}(\omega)\Gamma_\mathrm{R}(\omega)]\,, \tag{B9}$$

which, in the specific case of Sec. III, reads

$$g_{ij}^{-1K}(\omega) = 2\pi i\delta_{ij}\Gamma(\omega)[F_\mathrm{L}(\omega)\delta_{i,1}+F_\mathrm{R}(\omega)\delta_{i,N}]\,. \tag{B10}$$

Given the explicit dependence of the above expression on the distribution functions of the reservoirs $F_{\mathrm{L/R}}$, we can now perform the expansion in linear order in the chemical potential difference $\delta\mu = \mu_\mathrm{L}-\mu_\mathrm{R}$ to obtain the transmittance. We first show the linear expansion of the Keldysh component from Eq. (B5), whose diagonal terms read

$$i\frac{\mathcal{G}_i^K(\omega)}{2\pi} = \Gamma(\omega)U_i(\omega)+\gamma\mathcal{M}_{ij}(\omega)\left[\frac{1}{\mathbb{I}-M}\right]_{jk} \times\int\frac{d\omega'}{2\pi}\Gamma(\omega')U_k(\omega'), \tag{B11}$$

$$U_i(\omega) = F(\omega)V_i(\omega) - \frac{\delta\mu}{4T\cosh^2\left(\frac{\omega-\mu}{2T}\right)}W_i(\omega)\,, \tag{B12}$$

where we introduced the N dimensional vectors $V_i(\omega) = |\mathcal{G}_{i1}^R(\omega)|^2+|\mathcal{G}_{iN}^R(\omega)|^2$, $W_i(\omega) = |\mathcal{G}_{i1}^R(\omega)|^2-|\mathcal{G}_{iN}^R(\omega)|^2$ and $F(\omega) = \tanh[(\omega-\mu)/2T]$. Thanks to the mirror symmetry of the problem in Sec. III, the first term in Eq. (B12), proportional to the equilibrium distribution function F, does not contribute to the current given by the MW formula in Eq. (B4) and can be discarded. Assuming also $\mathcal{A}(\omega) = \mathcal{A}_{\mathrm{L/R}}(\omega)$, we thus find the following compact form for the transmittance in Eq. (15)

$$\mathcal{T}_\gamma(\omega) = 2\pi\Gamma(\omega)[\mathcal{A}(\omega)-\Delta^K(\omega)] \tag{B13}$$

with

$$\Delta^K(\omega) = [P(\omega)W(\omega)]_1 - [P(\omega)W(\omega)]_N\,, \tag{B14}$$

and

$$P(\omega) = \frac{\Gamma(\omega)}{2}+\frac{\gamma}{2}\int\frac{d\omega'}{2\pi}\Gamma(\omega')\mathcal{M}(\omega')\frac{1}{\mathbb{I}-M}\,, \tag{B15}$$

with the matrix $\mathcal{M}$ defined in Eq. (B7). In the case of a reservoir with a constant density of state, $\Gamma(\omega) = \Gamma$ and expression Eq. (B13) coincides with the one derived in Ref. [35].

Despite the general character of Eq. (B13), we note that, in purely one-dimensional systems, the current in the system equals the one flowing from the reservoirs to the system. As a consequence, we can extract a different, but equivalent, expression of the transmittance from performing similar manipulations as the ones described to derive Eq. (B13), but taking the local current expression Eq. (11) as a starting point. For this, the off-diagonal elements of $\mathcal{G}^K_{ij}(t=0)$ are needed, that can be readily obtained by injecting the solution (B6) for the diagonal elements into the Dyson equation (B5). Once taking the Fourier transform one finds

$$\mathcal{G}^K_{ij}(t=0) = iD_{ij} + i\gamma \int \frac{d\omega}{2\pi} \mathcal{G}^R_{il}(\omega) \left[\frac{1}{\mathbb{I} - M}\right]_{lm} D_m \mathcal{G}^A_{lj}(\omega). \tag{B16}$$

And the expression for the transmittance can be found from expanding D in the bias. The zeroth-order term in $\delta\mu$ does not contribute to the current, since without the bias the system is mirror symmetric and the current must be zero. Replacing the linear-order term of Eq. (B16) in Eq. (11) gives

$$\mathcal{T}_\gamma(\omega) = 2\pi t_x \Gamma(\omega) \mathrm{Im}\Bigg[\mathcal{G}^R_{i1}(\omega)\mathcal{G}^A_{1,i+1}(\omega) - \mathcal{G}^R_{iN}(\omega)\mathcal{G}^A_{N,i+1}(\omega) + \gamma \left[\frac{1}{\mathbb{I} - M}\right]_{lm} W_m(\omega) \int \frac{d\omega'}{2\pi} \mathcal{G}^R_{il}(\omega')\mathcal{G}^A_{l,i+1}(\omega')\Bigg]. \tag{B17}$$

The index i originates from computing the local current at site i but since the latter does not depend on the position, neither does the transmittance.

3. Average Lindblad description of the QSH dynamics

Lastly, we show how averaging a QSH over different noise realizations maps to a Lindblad evolution. Under the quantum stochastic evolution, the density matrix evolves as follows:

$$\begin{aligned}\rho_{t+dt} &= e^{-i(Hdt+dH_t)}\rho_t e^{-i(Hdt+dH_t)} \\ &= \rho_t - i[Hdt + dH_t, \rho_t] \\ &\quad + dH_t \rho_t dH_t - \frac{1}{2}\{dH_t^2, \rho_t\} + \mathcal{O}(dt^{3/2}), \\ &\approx \rho_t - i[Hdt + dH_t, \rho_t] \\ &\quad + \gamma \sum_{ijkl} (2c_i^\dagger c_j \rho_t c_k^\dagger c_l - \{c_k^\dagger c_l c_i^\dagger c_j, \rho_t\}) C_{ijkl} dt,\end{aligned} \tag{B18}$$

where we used the Itō rules and discarded terms of higher order than dt. The Lindblad equation is obtained by taking the noise-average of Eq. (B18), which sets the term proportional to dH_t to 0 in the Itō convention,

$$\frac{d}{dt}\rho_t = -i[H, \rho_t] + \gamma \sum_{ijkl} C_{ijkl}(2c_i^\dagger c_j \rho c_k^\dagger c_l - \{c_k^\dagger c_l c_i^\dagger c_j, \rho\}). \tag{B19}$$

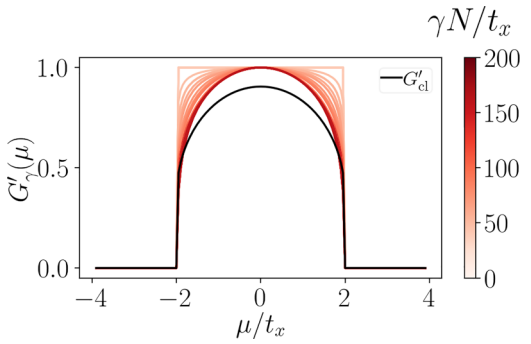

FIG. 7. Rescaled conductance profiles $G'_\gamma(\mu, N) := G_\gamma(\mu, N)/G_\gamma(0, N)$ for different values of γN with $\gamma = [0, 2]t_x$ and $N = [5, 200]$. The rescaled conductance converges in the diffusive limit $\gamma N/t_x \gg 1$ to a curve qualitatively similar to the semiclassical expectations in the same limit.

APPENDIX C: RESCALED CONDUCTANCE PROFILES

In this section, we present further numerical data on the conductance profiles in the diffusive regime. In this regime, the conductance decays with the inverse system size $G \propto 1/N$ thus, to focus on the chemical potential dependence, we depict in Fig. 7 the rescaled conductance $G'_\gamma(\mu, N) := G_\gamma(\mu, N)/G_\gamma(0, N)$ profiles for different values of γN and compare with the semiclassical rescaled value $G'_{\gamma,cl}(\mu, N) = G_{\gamma,cl}(\mu, N)/G_\gamma(0, N)$. The dependence of $G_\gamma(\mu = 0)$ on the system size N is plotted in Fig. 2. As we transition to the diffusive limit, the rescaled curves converge to a dome-like shape, which follows the qualitative dependence of the semiclassical approach, see black line for $G'_{\mathrm{cl}}(N \to \infty)$. The deviations between the exact and semiclassical approach are more significant in the center of the band but never exceed 10%.

We note that such strong dependence on the thermodynamic properties of the leads is not present in the diffusion constant and is a unique property of the conductance.

APPENDIX D: MIXING EFFECTS WITH DEPHASING NOISE

In this Appendix, we discuss the stationary state induced by dephasing noise on a one-dimensional tight-binding chain. We will qualitatively describe the out-of-equilibrium state reached by the dephased chain and show numerically on Fig. 8 that this qualitative intuition is correct. In the absence of dephasing, the whole chain will be in thermal equilibrium with a chemical potential and temperature matching the lead. Locally, it implies that the Green's functions satisfy the fluctuation dissipation relation

$$\mathcal{G}^K_{i,i}(\omega) = (1 - 2n_i(\omega))\big(\mathcal{G}^R_{i,i}(\omega) - \mathcal{G}^A_{i,i}(\omega)\big) \tag{D1}$$

with $n_i(\omega)$ the local Fermi distribution with parameters μ, T.

Beyond thermal equilibrium, we can still use Eq. (D1) as an *ad hoc* definition of $n_i(\omega)$ to characterize local deviations from equilibrium.

The presence of any dephasing rate drives the system out of equilibrium. As explained in the main text, the dephasing maximally mixes the longitudinal momentum states. Since

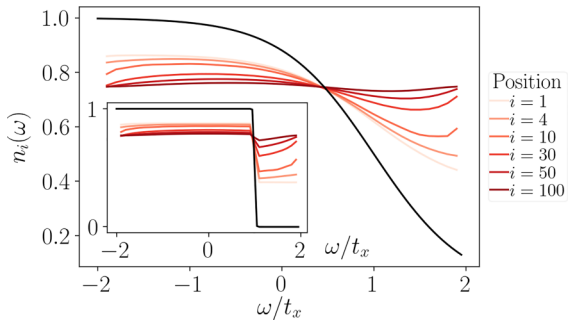

FIG. 8. Nonequilibrium local occupation distribution extracted from Eq. (D1) at different positions in a chain of $N = 200$ sites with on-site dephasing rate $\gamma = 0.05t_x$. The chain is coupled on the first and last site $i = 1, 200$ to a thermal lead with $\mu = t_x$ and $T = 0.5t_x$. The black line corresponds to the Fermi distribution of the attached reservoirs. (Inset) Same plot but the temperature of the leads is $T = 0.01t_x$.

these, in 1D, label all the eigenstates of the system the action of dephasing corresponds to heat the system to infinite temperature. However, since the dephasing terms commute with the local particle number operator, the attained steady-state preserves a well defined particle number. In other words, the local density matrix deep into a dephasing region resembles a thermal distribution with an effective μ^* and T^* such that $\mu^*, T^* \to \infty$ and μ^*/T^* tuned in such a way to have in the system the same spatial averaged particle density than the one in the attached leads.

This is clear in Fig. 8 where we plot $n_i(\omega)$ for different points in a dephasing chain coupled to a thermal lead on the left and right. By definition, the lead is in local thermal equilibrium and $n_{\mathrm{L,R}}(\omega)$ is given by the Fermi distribution, see black line. Near the lead, $n_i(\omega)$ deviates strongly from a thermal distribution indicating that the system is far from equilibrium. Deep into the chain, that is at distances from the leads larger than the scattering length ($i > t_x/\gamma$, in Fig. 8), $n(\omega)$ becomes flat as expected from a state with infinite μ, T. The exact ratio μ^*/T^* is uniquely determined from the density of the reservoirs but its exact value depends on the distribution of the system near the edges.

APPENDIX E: PROOF OF THE CONDITION (36)

In this Appendix, we give a proof of the condition Eq. (36) in the main text. The strategy is to write down the equations of motion for the total current of different noises and derive a condition under which they are equivalent (up to a factor) for different types of noise.

The action of the deterministic part H for the total current (11) evaluated at site j, is given for any site by

$$\partial_t J = i[H, J] = it_x^2 \sum_p [(n_{j+1,p} - n_{j,p}) + a^\dagger_{j-1,p} a_{j+1,p} - a^\dagger_{j,p} a_{j+2,p} - a^\dagger_{j+2,p} a_{j,p} + a^\dagger_{j+1,p} a_{j-1,p}]. \quad \text{(E1)}$$

Since H is quadratic, and since it doesn't mix the different modes by construction, its further action on quadratic operators will only generate terms of the type $a^\dagger_{j+k,p} a_{j+k,p'}$. By construction, the QSH (4) conserves the total number of particles at a given position on the x axis, i.e., $[dH_t, n_{j,\mathrm{tot}}] = 0$. Then, one sufficient but not necessary condition for the equations of motion to have the same form for all protocols is that the dual action on operators $\mathcal{L}^*$ for the averaged noise does not produce any new terms, i.e., we must have for $j \neq j'$

$$\mathcal{L}^*(a^\dagger_{j,p} a_{j',p}) = -\mathcal{N} a^\dagger_{j,p} a_{j',p}, \quad \text{(E2)}$$

where $\mathcal{N}$ is a constant, which depends on the type of noise we are interested in. Invoking the locality of the noise operator with respect to the longitudinal direction we have that

$$\mathcal{L}^*(a^\dagger_{j,p} a_{j',p}) = \mathcal{L}^*(a^\dagger_{j,p}) a_{j',p} + a^\dagger_{j,p} \mathcal{L}^*(a_{j',p}). \quad \text{(E3)}$$

So the sufficient condition (E2) can be cast into an even more restrictive one where we impose that $\forall p$, $(a^\dagger_{j,p}, a_{j,p})$ are eigenvectors of the operator $\mathcal{L}^*$.

Recall the explicit expression of $\mathcal{L}^*$

$$\mathcal{L}^*(\hat{O}) = \gamma \sum_{j, p_{1,2}, p'_{1,2}} C_{p_1,p'_1,p_2,p'_2} (2a^\dagger_{j,p_1} a_{j,p'_1} \hat{O} a^\dagger_{j,p_2} a_{j,p'_2} - \{a^\dagger_{j,p_1} a_{j,p'_1} a^\dagger_{j,p_2} a_{j,p'_2}, \hat{O}\}). \quad \text{(E4)}$$

Using that $C_{p_1,p'_1,p_2,p'_2} = C_{p'_1,p_1,p'_2,p_2}$, we have that

$$\mathcal{L}^*(a^\dagger_{j,p}) = -\gamma \sum_{p_1,p'} C_{p_1,p',p',p} a^\dagger_{j,p_1}, \quad \text{(E5)}$$

$$\mathcal{L}^*(a_{j,p}) = -\gamma \sum_{p_1,p'} C_{p',p_1,p,p'} a_{j,p_1}, \quad \text{(E6)}$$

and a sufficient condition for $(a^\dagger_{j,p}, a_{j,p})$ to be eigenvectors of $\mathcal{L}^*$ is then

$$\sum_p C_{p_1,p,p,p_2} = \mathcal{N} \delta_{p_1,p_2}, \quad \text{(E7)}$$

which is Eq. (36) of the main text.

For the coherent Noise I, one has $\mathcal{N} = 1$ and the transport properties of a given protocol model can be deduced from those of Noise I by rescaling the coefficient $\gamma \to \mathcal{N}\gamma$.

[1] E. Akkermans and G. Montambaux, *Mesoscopic Physics of Electrons and Photons* (Cambridge University Press, Cambridge, 2007)

[2] T. Giamarchi, Umklapp process and resistivity in one-dimensional fermion systems, Phys. Rev. B **44**, 2905 (1991).

[3] A. Rosch and N. Andrei, Conductivity of a Clean One-Dimensional Wire, Phys. Rev. Lett. **85**, 1092 (2000).

[4] J. Lux, J. Müller, A. Mitra, and A. Rosch, Hydrodynamic long-time tails after a quantum quench, Phys. Rev. A **89**, 053608 (2014).

[5] M. Medenjak, K. Klobas, and T. Prosen, Diffusion in Deterministic Interacting Lattice Systems, Phys. Rev. Lett. **119**, 110603 (2017).

[6] S. Gopalakrishnan and R. Vasseur, Kinetic Theory of Spin Diffusion and Superdiffusion in *XXZ* Spin Chains, Phys. Rev. Lett. **122**, 127202 (2019).

[7] A. J. Friedman, S. Gopalakrishnan, and R. Vasseur, Diffusive hydrodynamics from integrability breaking, Phys. Rev. B **101**, 180302(R) (2020).

[8] B. Bertini, F. Heidrich-Meisner, C. Karrasch, T. Prosen, R. Steinigeweg, and M. Žnidarič, Finite-temperature transport in one-dimensional quantum lattice models, Rev. Mod. Phys. **93**, 025003 (2021).

[9] T. Prosen, Open *XXZ* Spin Chain: Nonequilibrium Steady State and a Strict Bound on Ballistic Transport, Phys. Rev. Lett. **106**, 217206 (2011).

[10] T. Prosen, Exact Nonequilibrium Steady State of a Strongly Driven Open *XXZ* Chain, Phys. Rev. Lett. **107**, 137201 (2011).

[11] D. Karevski and T. Platini, Quantum Nonequilibrium Steady States Induced By Repeated Interactions, Phys. Rev. Lett. **102**, 207207 (2009).

[12] D. Karevski, V. Popkov, and G. M. Schütz, Exact Matrix Product Solution for the Boundary-Driven Lindblad *XXZ* Chain, Phys. Rev. Lett. **110**, 047201 (2013).

[13] J. S. Ferreira and M. Filippone, Ballistic-to-diffusive transition in spin chains with broken integrability, Phys. Rev. B **102**, 184304 (2020).

[14] T. Jin, M. Filippone, and T. Giamarchi, Generic transport formula for a system driven by Markovian reservoirs, Phys. Rev. B **102**, 205131 (2020).

[15] M. Žnidarič, Exact solution for a diffusive nonequilibrium steady state of an open quantum chain, J. Stat. Mech. (2010) L05002.

[16] B. Bertini, M. Collura, J. De Nardis, and M. Fagotti, Transport in Out-Of-Equilibrium *XXZ* Chains: Exact Profiles of Charges and Currents, Phys. Rev. Lett. **117**, 207201 (2016).

[17] T. Müller, M. Gievers, H. Fröml, S. Diehl, and A. Chiocchetta, Shape effects of localized losses in quantum wires: Dissipative resonances and nonequilibrium universality, Phys. Rev. B **104**, 155431 (2021).

[18] D. Rossini, A. Ghermaoui, M. B. Aguilera, R. Vatré, R. Bouganne, J. Beugnon, F. Gerbier, and L. Mazza, Strong correlations in lossy one-dimensional quantum gases: From the quantum zeno effect to the generalized Gibbs ensemble, Phys. Rev. A **103**, L060201 (2021).

[19] V. Alba and F. Carollo, Noninteracting fermionic systems with localized losses: Exact results in the hydrodynamic limit, Phys. Rev. B **105**, 054303 (2022).

[20] A. M. Visuri, T. Giamarchi, and C. Kollath, Symmetry-Protected Transport Through a Lattice with a Local Particle Loss, Phys. Rev. Lett. **129**, 056802 (2022).

[21] M. Žnidarič, Dephasing-induced diffusive transport in the anisotropic Heisenberg model, New J. Phys. **12**, 043001 (2010).

[22] A. Bastianello, J. De Nardis, and A. De Luca, Generalized hydrodynamics with dephasing noise, Phys. Rev. B **102**, 161110(R) (2020).

[23] V. Eisler, Crossover between ballistic and diffusive transport: the quantum exclusion process, J. Stat. Mech. (2011) P06007.

[24] P. E. Dolgirev, J. Marino, D. Sels, and E. Demler, Non-Gaussian correlations imprinted by local dephasing in fermionic wires, Phys. Rev. B **102**, 100301(R) (2020).

[25] D. Wellnitz, G. Preisser, V. Alba, J. Dubail, and J. Schachenmayer, The Rise and Fall, and Slow Rise Again, of Operator Entanglement Under Dephasing, Phys. Rev. Lett. **129**, 170401 (2022).

[26] M. Bauer, D. Bernard, and T. Jin, Equilibrium fluctuations in maximally noisy extended quantum systems, SciPost Phys. **6**, 045 (2019).

[27] D. Bernard and T. Jin, Open Quantum Symmetric Simple Exclusion Process, Phys. Rev. Lett. **123**, 080601 (2019).

[28] T. Jin, A. Krajenbrink, and D. Bernard, From Stochastic Spin Chains to Quantum Kardar-Parisi-Zhang Dynamics, Phys. Rev. Lett. **125**, 040603 (2020).

[29] F. H. L. Essler and L. Piroli, Integrability of one-dimensional lindbladians from operator-space fragmentation, Phys. Rev. E **102**, 062210 (2020).

[30] D. Bernard and L. Piroli, Entanglement distribution in the quantum symmetric simple exclusion process, Phys. Rev. E **104**, 014146 (2021).

[31] D. Bernard and P. L. Doussal, Entanglement entropy growth in stochastic conformal field theory and the KPZ class, Europhys. Lett. **131**, 10007 (2020).

[32] M. V. Medvedyeva, F. H. L. Essler, and T. Prosen, Exact Bethe Ansatz Spectrum of a Tight-Binding Chain with Dephasing Noise, Phys. Rev. Lett. **117**, 137202 (2016).

[33] M. Bauer, D. Bernard, and T. Jin, Stochastic dissipative quantum spin chains (I) : Quantum fluctuating discrete hydrodynamics, SciPost Phys. **3**, 033 (2017).

[34] X. Turkeshi and M. Schiró, Diffusion and thermalization in a boundary-driven dephasing model, Phys. Rev. B **104**, 144301 (2021).

[35] T. Jin, J. S. Ferreira, M. Filippone, and T. Giamarchi, Exact description of quantum stochastic models as quantum resistors, Phys. Rev. Research **4**, 013109 (2022).

[36] J. De Nardis, S. Gopalakrishnan, E. Ilievski, and R. Vasseur, Superdiffusion from Emergent Classical Solitons in Quantum Spin Chains, Phys. Rev. Lett. **125**, 070601 (2020).

[37] C. Zu, F. Machado, B. Ye, S. Choi, B. Kobrin, T. Mittiga, S. Hsieh, P. Bhattacharyya, M. Markham, D. Twitchen, A. Jarmola *et al.*, Emergent hydrodynamics in a strongly interacting dipolar spin ensemble, Nature (London) **597**, 45 (2021).

[38] J. Wurtz, P. W. Claeys, and A. Polkovnikov, Variational Schrieffer-Wolff transformations for quantum many-body dynamics, Phys. Rev. B **101**, 014302 (2020).

[39] J. D. Nardis, D. Bernard, and B. Doyon, Diffusion in generalized hydrodynamics and quasiparticle scattering, SciPost Physics **6**, 049 (2019).

[40] R. Steinigeweg, F. Heidrich-Meisner, J. Gemmer, K. Michielsen, and H. De Raedt, Scaling of diffusion constants in the spin-1/2 XX ladder, Phys. Rev. B **90**, 094417 (2014).

[41] N. Dogra, M. Landini, K. Kroeger, L. Hruby, T. Donner, and T. Esslinger, Dissipation-induced structural instability and chiral dynamics in a quantum gas, Science **366**, 1496 (2019).

[42] F. Ferri, R. Rosa-Medina, F. Finger, N. Dogra, M. Soriente, O. Zilberberg, T. Donner, and T. Esslinger, Emerging Dissipative Phases in a Superradiant Quantum Gas with Tunable Decay, Phys. Rev. X **11**, 041046 (2021).

[43] R. Rosa-Medina, F. Ferri, F. Finger, N. Dogra, K. Kroeger, R. Lin, R. Chitra, T. Donner, and T. Esslinger, Observing Dynamical Currents in a Non-Hermitian Momentum Lattice, Phys. Rev. Lett. **128**, 143602 (2022).

[44] L. Corman, P. Fabritius, S. Häusler, J. Mohan, L. H. Dogra, D. Husmann, M. Lebrat, and T. Esslinger, Quantized conductance through a dissipative atomic point contact, Phys. Rev. A **100**, 053605 (2019).

[45] M. Lebrat, S. Häusler, P. Fabritius, D. Husmann, L. Corman, and T. Esslinger, Quantized Conductance Through a Spin-Selective Atomic Point Contact, Phys. Rev. Lett. **123**, 193605 (2019).

[46] M. Mancini, G. Pagano, G. Cappellini, L. Livi, M. Rider, J. Catani, C. Sias, P. Zoller, M. Inguscio, M. Dalmonte, and L. Fallani, Observation of chiral edge states with neutral fermions in synthetic Hall ribbons, Science **349**, 1510 (2015).

[47] D. Genkina, L. M. Aycock, H.-I. Lu, M. Lu, A. M. Pineiro, and I. Spielman, Imaging topology of Hofstadter ribbons, New J. Phys. **21**, 053021 (2019).

[48] T. Chalopin, T. Satoor, A. Evrard, V. Makhalov, J. Dalibard, R. Lopes, and S. Nascimbene, Probing chiral edge dynamics and bulk topology of a synthetic Hall system, Nat. Phys. **16**, 1017 (2020).

[49] T. W. Zhou, G. Cappellini, D. Tusi, L. Franchi, J. Parravicini, C. Repellin, S. Greschner, M. Inguscio, T. Giamarchi, M. Filippone, J. Catani, and L. Fallani, Observation of universal Hall response in strongly interacting fermions, arXiv:2205.13567.

[50] B. Øksendal, *Stochastic Differential Equations* (Springer, Berlin, 2003).

[51] A. Kamenev, *Field Theory of Non-Equilibrium Systems* (Cambridge University Press, Cambridge, 2011) pp. 1–341.

[52] The Green's functions depend on the time differences $t - t'$, instead of separate times t, t', as we consider situations where both the Hamiltonian (1) and Lindblad generator (6) do not depend explicitly on time.

[53] A. I. Larkin and I. N. Ovchinnikov, Nonlinear effects during vortex motion in superconductors, Zh. Eksp. Teor. Fiz. **73**, 299 (1977).

[54] R. Landauer, Spatial variation of currents and fields due to localized scatterers in metallic conduction, IBM J. Res. Dev. **1**, 223 (1957).

[55] S. Datta, *Electronic Transport in Mesoscopic Systems* (Cambridge University Press, Cambridge, 1997).

[56] G. B. Lesovik and I. A. Sadovskyy, Scattering matrix approach to the description of quantum electron transport, Phys. Usp. **54**, 1007 (2011).

[57] Y. V. Nazarov and Y. M. Blanter, *Quantum Transport: Introduction to Nanoscience* (Cambridge University Press, Cambridge, 2009).

[58] M. Žnidarič and M. Horvat, Transport in a disordered tight-binding chain with dephasing, Eur. Phys. J. B **86**, 67 (2013).

[59] Z. Cai and T. Barthel, Algebraic Versus Exponential Decoherence in Dissipative Many-Particle Systems, Phys. Rev. Lett. **111**, 150403 (2013).

[60] Despite the possibility to rely on Eq. (15) to calculate the conductance for $\gamma > 0$, we found more practical to perform the direct numerical calculation of the current as expressed in Eq. (11) directly in the linear regime to derive the conductance (12).

[61] The different scalings of D and G with μ, T indicate that the contact resistance between bulk and leads is extensive with the system size. Fig. 8 and previous papers [34] suggest that thermalization only occurs very deep in the bulk, supporting this hypothesis.

[62] J. Dalibard, Y. Castin, and K. Mølmer, Wave-Function Approach to Dissipative Processes in Quantum Optics, Phys. Rev. Lett. **68**, 580 (1992).

[63] V. Belavkin, A quantum stochastic calculus in fock space of input and output nondemolition processes, J. Sov. Math. v, 99 (1990).

[64] Convergence is exponential with the number of iterations and independent of the initial guess for $P(x)$, which we take arbitrarily.

[65] X. Cao, A. Tilloy, and A. D. Luca, Entanglement in a fermion chain under continuous monitoring, SciPost Phys. **7**, 024 (2019).

[66] X. Turkeshi, M. Dalmonte, R. Fazio, and M. Schirò, Entanglement transitions from stochastic resetting of non-Hermitian quasiparticles, Phys. Rev. B **105**, L241114 (2022).

[67] G. Salerno, H. M. Price, M. Lebrat, S. Häusler, T. Esslinger, L. Corman, J.-P. Brantut, and N. Goldman, Quantized Hall Conductance of a Single Atomic Wire: A Proposal Based on Synthetic Dimensions, Phys. Rev. X **9**, 041001 (2019).

[68] L. F. Livi, G. Cappellini, M. Diem, L. Franchi, C. Clivati, M. Frittelli, F. Levi, D. Calonico, J. Catani, M. Inguscio, and L. Fallani, Synthetic Dimensions and Spin-Orbit Coupling with an Optical Clock Transition, Phys. Rev. Lett. **117**, 220401 (2016).

[69] T. Ozawa, H. M. Price, N. Goldman, O. Zilberberg, and I. Carusotto, Synthetic dimensions in integrated photonics: From optical isolation to four-dimensional quantum hall physics, Phys. Rev. A **93**, 043827 (2016).

[70] S. Mittal, V. V. Orre, D. Leykam, Y. D. Chong, and M. Hafezi, Photonic Anomalous Quantum Hall Effect, Phys. Rev. Lett. **123**, 043201 (2019).

[71] R. A. Usmani, Inversion of a tridiagonal Jacobi matrix, Linear Algebra Appl. **212-213**, 413 (1994).

[72] Y. Meir and N. S. Wingreen, Landauer Formula for the Current Through an Interacting Electron Region, Phys. Rev. Lett. **68**, 2512 (1992).